High Temperature Thermal Physical Properties of High-alumina Fibrous Insulation

Boming ZHANG, Shuyuan ZHAO†, Xiaodong HE and Shanyi DU

Center for Composite Materials and Structure, Harbin Institute of Technology, Harbin 150080, China

The thermal properties of high-alumina fibrous insulation which filled in metallic thermal protection system were investigated. The effective thermal conductivities of the fibrous insulation were measured under an atmospheric pressure from 10^{-2} to 10^5 Pa. In addition, the changes of the specific heat and Rosseland mean extinction coefficient were experimentally determined under various surrounding temperatures up to 973 K. The spectral extinction coefficients were obtained from transmittance data in the wavelength range of 2.5–25 μm using Beer's law. Rosseland mean extinction coefficients as a function of temperature were calculated based on spectral extinction coefficients at various temperatures. The results show that thermal conductivities of the sample increase with increasing temperature and pressure. Specific heat increases as temperature increases, which shows that the capacity of heat absorption increases gradually with temperature. Rosseland mean extinction coefficients of the sample decrease firstly and then increase with increasing the temperature.

KEY WORDS: Effective thermal conductivity; Extinction coefficient; Transmittance; Thermal physical properties

1. Introduction

Space transportation vehicles entering the earth's atmosphere at hypersonic speeds encounter aerodynamic heating. Thermal protective system is usually required to limit the maximum temperature of the primary structure of the vehicle during entry. A metallic thermal protective system consists of a metallic shell panel fabricated from high temperature alloy and the lightweight, non-load-bearing insulation. High temperature fibrous insulation is attached much importance for its low density, excellent heat-insulated properties and high service temperature, and it becomes the insulation candidate being considered for use in the metallic thermal protection system on reusable launch vehicles. The service environment for the insulation of the current metallic TPS (thermal protection system) is complex: the environmental pressure varies from 1.333 to 1.013×10^5 Pa, while the hot surface of insulation is exposed to temperature as high as 1273 K[1]. Low effective thermal conductivity for the insulation can maintain the temperature of the main structure within acceptable limits. Higher heat capacity of the insulation is more favorable in terms of high temperature application. The temperature field will be uniform with more heat energy contained or absorbed by the material, which helps to avoid failure caused by excessive thermal stress. In addition, at high temperature, radiation heat transfer is more dominant due to the fact that it is proportional to the fourth power of temperature. Therefore, its local radiative property, that is the extinction coefficient as a parameter of radiation heat transfer, becomes more and more important. However, limited information is available on the thermal properties of insulation under the environmental conditions to which re-entry type vehicles are exposed. Therefore, investigations on thermal physical properties for insulation are needed to ensure the safety of structure.

Over the past several decades, significant advances have been made in the understanding of fundamental properties of fibrous insulation materials[2–5]. Thermal test techniques are broadly classified under steady state methods and transient methods. Among the steady state methods, the guarded hot plate (GHP) may be regarded as the most commonly used technique for measuring the thermal conductivity of insulation materials. The NASA Langley Research Center developed an experimental apparatus to measure the apparent thermal conductivity of insulation under steady-state conditions based on the ASTM C-201 standard[6]. The main difference between the apparatus and the ASTM standard is that thin foil heat flux gages are used for measuring the heat flux, while three guarded water calorimeters are used in the ASTM standard. The apparatus can provide apparent thermal conductivity of specimen with cold side temperature maintained around room temperature, and specimen with hot side temperatures up to 1273 K at environmental pressures from 1.333×10^{-2} to 1.013×10^5 Pa.

Although there have been several steady-state standard methods, such as YB/T 4130-2005[7] and GB/T 17911.8-2002[8], to measure the thermal conductivity of fibrous insulation in China, these approaches were not suitable for simulating desired test conditions with large temperature gradients across the sample. In the present study, an apparatus was developed based on the test demands of the fibrous insulation under conditions experienced during re-entry aerodynamic heating. Effective thermal conductivity of high-alumina fibrous insulation was measured at pressures from 10^{-2} to 10^5 Pa, and temperatures up to 973 K using the developed apparatus. Specific heat of the sample was also measured at the corresponding range of temperatures. The spectral transmittance of the sample in the wavelength range of 2.5–25 μm was measured using a Fourier transform infrared spectrometer (FTIR). The extinction coefficient was obta-

Table 1 Nominal chemical composition of
high-alumina fibrous insulation

Chemical composition	Content/wt pct
Al_2O_3	52–55
Al_2O_3+SiO_2	98
Fe_2O_3	0.25
R_2O	0.25
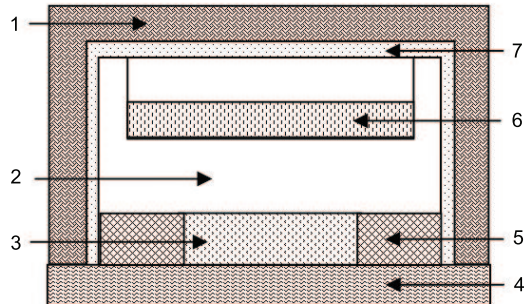
Fig.1 Schematic of the thermal conductivity apparatus:
1—carbon fabric insulation barrel, 2—vacuum
chamber, 3—test specimen, 4—water-cooled
plate, 5—guarded insulation, 6—graphite radiant
heater, 7—insulating screen

ined from transmittance data using Beer′s law. Based
on spectral extinction coefficients at various temper-
atures, Rosseland mean extinction coefficients as a
function of temperature were calculated. The research
provides important new contributions to analysis and
design of insulation for re-entry aerodynamic heating
conditions.

2. Sample Description

The fibrous insulation sample studied in this in-
vestigation was high-alumina fibrous insulation. Its
primary components are alumina and silica. Nominal
chemical composition of the insulation is listed in Ta-
ble 1. Melting point of the fiber is around 2030 K.
Continuous service temperature is 1473 K. The mean
diameter of the fiber is 5×10^{-6} m. The nominal den-
sity is 128 kg/m^3.

3. Experimental Methodology

3.1 Effective thermal conductivity
Effective thermal conductivity, which combines
the effects of heat transfer by conduction, convec-
tion, and radiation, is one of the most important pa-
rameters to characterize the thermal performance of
the insulation. Effective thermal conductivity varies
with temperature and pressure under the aerody-
namic heating conditions. In order to investigate
heat transfer through fibrous insulation and obtain
the effective thermal conductivity of insulation sam-
ple exactly and reliably, an apparatus was developed
to measure the steady-state effective thermal conduc-
tivity of the insulation. A schematic of the apparatus
(high-temperature graphite plate furnace) is shown in
Fig.1. The sample is placed between a graphite radi-
ant heater that can reach a temperature as high as
1873 K and a water-cooled plate maintaining room
temperature. The water-cooled plate is placed on

the bottom to reduce the effect of natural convec-
tion. Thermocouples are installed at strategic loca-
tions to monitor the change of temperature distribu-
tion throughout the specimen during heating. Heat
flux gauges located on the water-cooled plate are used
to measure the flux of heat energy flowing through
the sample. The apparatus is located inside a vac-
uum chamber and the environmental pressure varies
between 10^{-2} and 10^5 Pa. Once the insulation sam-
ple is inserted into the test apparatus, the gas inside
the vacuum chamber is removed. The primary rea-
son for selecting N_2 as atmosphere gas in this exper-
iment is to eliminate the water vapor in the chamber
and to weaken the oxidation of the graphite at higher
temperature. Once all the thermocouples on the hot
side and the cold side and the heat flux gages on the
water-cooled plate are stabilized, data storage is ini-
tiated. Using the measured heat flux, the hot side
temperature, the cold side temperature, and sample
thickness, the effective thermal conductivity, k_e of the
insulation sample can be calculated by Fourier′s law
of heat conduction:

$$k_e = \frac{qL}{T_1 - T_2} \quad (1)$$

where q is the measured heat flux, L is the insulation
thickness, and T_1 and T_2 are the measured tempera-
tures on the hot side and cold side, respectively.

The uncertainty of the measurement is estimated
from the error propagation equation of Eq.(2).

$$\frac{\delta k}{k_e} = \left(\left(\frac{\delta q}{q}\right)^2 + \left(\frac{\delta L}{L}\right)^2 + \left(\frac{\delta \Delta T}{\Delta T}\right)^2\right)^{0.5} \quad (2)$$

The uncertainty of the measured effective thermal
conductivity is 8% approximately.

In the present study, the sample has a square cross
sectional area with the sides being 450 mm. The nom-
inal thickness of the sample is 40 mm. The effective
thermal conductivity of the sample is measured with
the nominal hot side temperatures of 373, 473, 573,
673, 773, 873 and 973 K, and the nominal experimen-
tal pressures controlled at 1×10^{-2}, 5, 30, 6.5×10^3,
5.13×10^4 and 1.013×10^5 Pa. Each measurement con-
sists of setting the temperature of the top of the sam-
ple to the desired temperature, varying the N_2 gas to
the desired pressure, and allowing both the tempera-
ture and the pressure to reach a steady state.

3.2 Specific heat
Specific heat is not only one of the most impor-
tant thermal physical properties of insulation, which
are used in heat energy calculations and designs, but
also an important parameter used in the evaluation
of the materials, especially for thermal protective and
heat-insulated materials.

In the present study, specific heat was measured
with a thermal analysis system (NETZSCH STA
449C, Germany). The measuring principle is to com-
pare the rate of heat flow to the sample with that to a
reference at the programmed temperature. Whether
more or less heat must flow to the sample depends on
whether the process is exothermic or endothermic. If
the difference in heat flow between the sample and the
reference is detected, from the mass of the sapphire
standard, the known specific heat of sapphire, and the
data signals collected from DSC (differential scanning

calorimetry), the specific heat of sample, Cp_{sam} can be calculated.

$$Cp_{\text{sam}} = Cp_{\text{std}} \frac{\frac{DSC_{\text{sam}} - DSC_{\text{bsl}}}{M_{\text{sam}}}}{\frac{DSC_{\text{std}} - DSC_{\text{bsl}}}{M_{\text{std}}}} \qquad (3)$$

where DSC_{bsl} is the measured DSC signal of baseline; DSC_{std} is the measured DSC signal of standard (sapphire); DSC_{sam} is the measured DSC signal of sample; M_{sam} is mass of sample; and Cp_{std} is the specific heat of standard.

The sample was ground into powder before measured. The specific heat of sample was measured for the temperature range of 323–973 K at a heating rate of 3 K/min under Ar atmosphere. The mass of the sample used for experiment was 17.69 mg.

3.3 Rosseland mean extinction coefficient

To study the thermal radiation within insulation, its local radiative property, that is the extinction coefficient, is needed. Physically, the extinction coefficient represents the decay rate of the radiation intensity passing through the material. For engineering applications, the Rosseland mean extinction coefficient is a more commonly used material parameter than the spectral extinction coefficient, as the former represents the overall effect of energy decay in the material. The Rosseland mean extinction coefficient is defined as[9]:

$$\frac{1}{K_{\text{R}}} = \frac{\int_0^\infty \frac{1}{\beta_\lambda} \frac{\partial e_{\text{b}\lambda}}{\partial T} d\lambda}{\int_0^\infty \frac{\partial e_{\text{b}\lambda}}{\partial T} d\lambda} = \int_0^\infty \frac{1}{\beta_\lambda} \frac{\partial e_{\text{b}\lambda}}{\partial e_{\text{b}}} d\lambda \qquad (4)$$

where λ is the wavelength, T is the medium temperature; e_{b} is the blackbody emissive power; $e_{\text{b}\lambda}$ is the spectral black body emissive power, and β_λ is the spectral extinction coefficient. The spectral extinction coefficients for thin sample can be obtained by using Beer's law[10]:

$$T_{n\lambda} = \exp\left(-\int_0^L \beta_\lambda dx\right) \qquad (5)$$

where $T_{n\lambda}$ is the spectral transmittance and L is the thickness of the sample. For a homogeneous sample, β_λ is independent of the sample thickness, then Eq.(5) can be reduced to:

$$\beta_\lambda = -\frac{\ln(T_{n\lambda})}{L} \qquad (6)$$

For black bodies, the monochromatic emissive power was derived by Planck by introducing the quantum concept for electromagnetic energy as:

$$e_{\text{b}\lambda} = \frac{C_1 \lambda^{-5}}{e^{C_2/\lambda T} - 1} \qquad (7)$$

where $C_1 = 3.743 \times 10^{-16}$ W·m^2 and $C_2 = 1.4387 \times 10^{-2}$ m·K.

By integrating Planck's law over the wavelength, it has been established that over 50% of the thermal radiation lies in the wavelength range of 2.5–25 μm below 973 K. In this study, the spectral transmittance was measured for the wavelength range of 2.5–25 μm using a Fourier transform infrared spectrometer (FTIR, Bruker IFS 66 V/s, Germany).
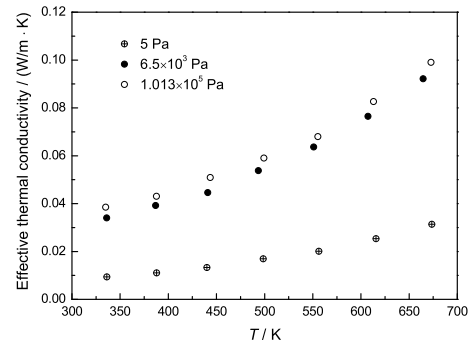

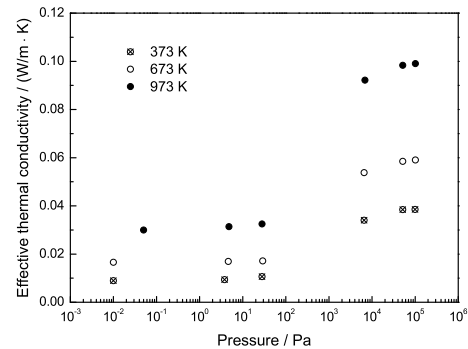**Fig.2** Variation of effective thermal conductivity with temperature

Fig.3 Variation of effective thermal conductivity with pressure

4. Results and Discussion

4.1 Effective thermal conductivity

The heat transfer mechanisms in fibrous insulation include solid conduction, gas conduction and radiation. Convection heat transfer is negligible. The effective thermal conductivity as a function of sample average temperature is shown in Fig.2. The effective thermal conductivity increases non-linearly with increasing sample average temperature, due to the fact that radiation heat transfer is related to the fourth power of temperature, and it is more dominant with the increase in temperature.

To gain further insight into the influence of environmental pressure on the overall heat transfer, the variation of effective thermal conductivity with environmental pressure for the sample is shown in Fig.3. Data are plotted for three different nominal hot side temperatures. The figure shows that the measured effective thermal conductivity for each sample average temperature increases with increasing pressure. As can be seen, the effective thermal conductivity increases, more rapidly between 30 Pa and 6.5×10^3 Pa than that below 5 Pa, and then stays relatively constant above 5.132×10^4 Pa. This trend is in accordance with the relevant experimental results in literature [4]. As solid and radiative contributions are independent of gas pressure, changing pressure only affects the contribution of gas conduction to the effective thermal conductivity. It can be stated that gas conduction increases with increasing pressure. The same trends are observed for all other insulation samples.
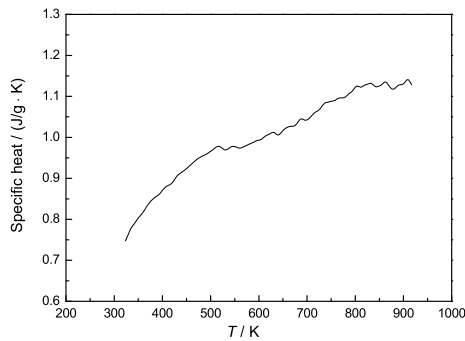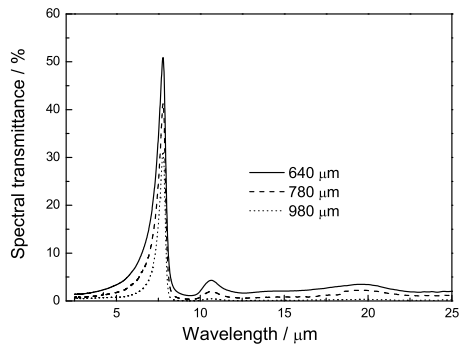
Fig.4 Variation of specific heat with temperature

Fig.5 Variation of spectral transmission of samples with different thicknesses and wavelength at room temperature

Fig.6 Variation of spectral transmittance of samples with wavelength at various temperatures

4.2 Specific heat

Figure 4 presents the variation of the specific heat of fibrous insulation sample with temperature. No sharp peaks can be observed in Fig.4, which indicates that no phase transformation occurs for the investigated temperature range. The specific heat of sample increases with increasing temperature. The rate increases rapidly below 800 K, and then increases slightly. Given the same temperature rise, heat consumption increases with temperature. The ability of heat absorption for insulation sample enhances with increasing temperature. This is the predominance of fibrous insulation to be used as high temperature heat-insulation materials.

4.3 Rosseland mean extinction coefficient

The measured spectral transmittance is plotted as a function of wavelength in Fig.5 for high-alumina fibrous insulation with different thicknesses. The results of Fig.5 demonstrate that the spectral transmittance decreases as the media thickness increases. The insulation transmittance property is strongly dependent upon the spectral wavelength. The transmittance initially increases with increasing wavelength and decreases sharply to reach the first absorption peak at around 9 μm, and then increases somewhat before decreasing again. The second absorption peak is reached at around 12 μm. Afterward the transmittance gradually increases and reaches a plateau. It is noticed that all the three testing samples with different thicknesses exhibit similar dependence upon the wavelength. The spectral transmittance of the samples *vs* wavelength relation is determined
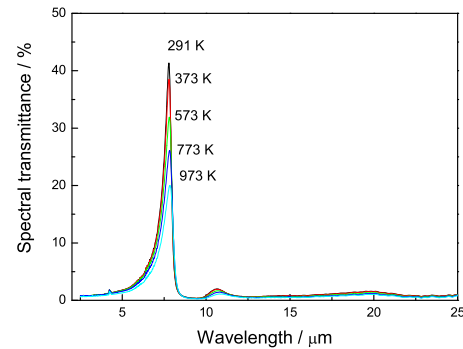
mainly by the insulation microstructures and solid material properties. When irradiated by infrared ray, the sample will absorb optical energy if the vibration or rotation frequency of some chemical bond in the sample corresponds to the frequency of the infrared ray, causing the variation of permanent molecular dipole moment, which leads to the vibration and rotation energy transition from ground state to excited state, and thus weakens the intensity of transmitted light of the corresponding frequency. The absorbed peak at the wavelength of 9 μm is related to antisymmetric stretching vibration of Si-O-Si bond and the absorbed peak at the wavelength of 12 μm is related to symmetric stretching vibration of Si-O-Si bond.

Figure 6 shows the variation of spectral transmittance of samples with wavelength at various temperatures. Given the fact that there is no obvious change in the physical and chemical properties of high-alumina fibrous insulation up to 973 K, the trends are similar for the sample at various temperatures. The maximum values of transmittance decrease and show a shift towards the direction of longer wavelength as temperature increases. It can be explained by the fact that spectral transmittance is the ratio of spectral intensity after and before the insulation sample of thickness. According to Plank's law, emissive power increases and the maximum of emissive power shows a shift towards the direction of shorter wavelength with increasing temperature, therefore spectral intensity decreases after it goes through the insulation sample of a certain thickness and shows a shift towards the direction of longer wavelength with increasing temperature.

Spectral extinction coefficient can be obtained from Eq.(5) using the spectral transmittance. The spectral extinction coefficient thus determined is plotted as a function of wavelength in Figs.7 and 8. Figure 7 shows that there is a little fluctuation in the spectral extinction coefficients of samples with different thicknesses because of the error of thickness measuring and the scattering effects. Figure 8 demonstrates that the spectral extinction coefficients of samples at various temperatures exhibit similar trend. Spectral extinction coefficients increase slightly as temperature increases. If the thickness of the sample is sufficiently large, the optical thickness (the optical thickness equals to extinction coefficient plus thickness of the sample) of the insulation will be large enough for the sample to be treated as an optically
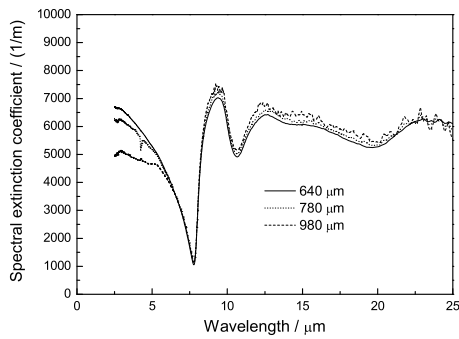
Fig.7 Variation of spectral extinction coefficient of samples with different thicknesses and wavelength at room temperature
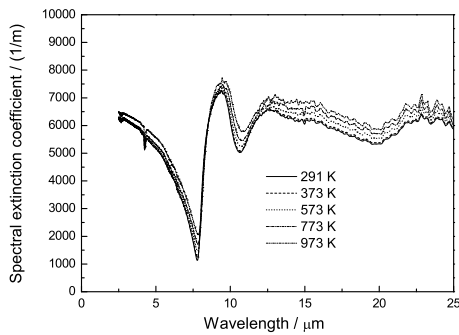

Fig.8 Variation of spectral extinction coefficient of samples with wavelength at various temperatures
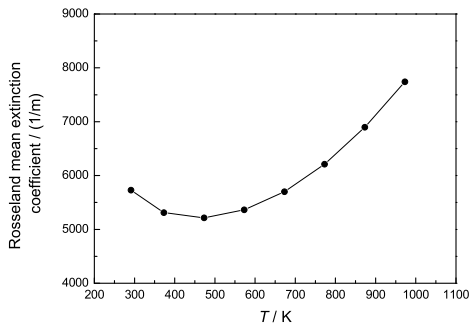

Fig.9 Variation of Rosseland mean extinction coefficient with temperature

thick medium, and radiation in the insulation can be considered as a diffusion process.

Rosseland mean extinction coefficient is an average extinction coefficient over the spectrum weighted by the emissive power. It represents the ability to eliminate thermal radiation at a certain temperature. The variation of Rosseland mean extinction coefficient with temperature obtained from Eq.(4) is shown in Fig.9. The results demonstrate that the Rosseland mean extinction coefficient initially decreases with increasing temperature, reachs the minimum value of 5216 l/m at around 573 K, and then increases with the temperature. The radiative thermal conductivity, k_r for an optically thick medium can be obtained from $k_r = \frac{16\sigma}{3K_R}T^3$ (σ is the Stefan-Boltzmann

constant). Therefore the Rosseland mean extinction coefficients obtained by this experimental method will provide advantageous basis and data references to better understand the mechanism of radiative heat transfer in fibrous insulation.

5. Conclusion

This paper presented the experimental study of thermal performances of high-alumina fibrous insulation. Effective thermal conductivity of high-alumina fibrous insulation subjected to large temperature differences was measured. The hot side of the insulation sample was heated to temperatures up to 973 K. The environmental pressure varied from 10^{-2} to 10^5 Pa. It was found that effective thermal conductivity of samples increased non-linearly with the temperature due to the non-linearity of radiation heat transfer. The contribution of gas conduction to overall heat transfer made effective thermal conductivity increase with experimental pressures. The specific heat of sample increased with the temperature. The ability of heat absorption for insulation sample enhances with the temperature. The spectral transmittance of the insulation sample was measured, which was then used to determine the spectral extinction coefficient and Rosseland mean extinction coefficient. It was found that the spectral quantities were strongly dependent on the wavelength. The Rosseland mean extinction coefficient initially decreased and then increased with increasing temperature. The research provides new important contributions to the analysis and design of insulation for re-entry aerodynamic heating conditions.

REFERENCES

[1] K.Daryabeigi: Ph.D. Thesis, University of Virginia, USA, 2000, 5.
[2] T.W.Tong, S.Q.Yang and C.L.Tien: *J. Heat Transfer,* 1983, **105**(1), 70.
[3] J.D.Verschoor, P.Greebler and N.J.Manville: *J. Heat Transfer,* 1952, **74,** 467.
[4] K.Daryabeigi: *NASA/TM,* 1999, 2.
[5] N.E.Hager and R.C.Steere: *J. Appl. Phys.,* 1967, **38**(12), 4663.
[6] K.Daryabeigi: *AIAA* 99-1044.
[7] Chinese Metallurgical Standards: YB/T 4130-2005. (in Chinese)
[8] Chinese National Standards: GB/T 17911.8-2002. (in Chinese)
[9] V.Giaretto, E.Miraldi and G.Ruscica: *High Temp. High Press,* 1995/1996, (27/28), 191.
[10] R.Siegel and J.R.Howell: *Thermal Radiation Heat Transfer,* Taylor & Francis, London, 1992.